

Spectroscopy of ^{13}B , ^{14}B , ^{15}B and ^{16}B using multi-nucleon transfer reactions

R. Kalpakchieva^{1,a}, H.G. Bohlen², W. von Oertzen², B. Gebauer², M. von Lucke-Petsch², T.N. Massey³, A.N. Ostrowski⁴, Th. Stolla², M. Wilpert², Th. Wilpert²

¹ Flerov Laboratory of Nuclear Reactions, JINR, 141980 Dubna, Moscow region, Russia

² Hahn-Meitner Institut GmbH, Glienicke Strasse 100, 14109 Berlin, Germany

³ Department of Physics and Astronomy, Ohio University, Athens, OH 45701-2979, USA

⁴ Department of Physics and Astronomy, The University of Edinburgh, Edinburgh, EH9 3J2, UK

Received: 27 December 1999 / Revised version: 11 February 2000

Communicated by D. Schwalm

Abstract. New information has been obtained on excited states of the neutron-rich boron isotopes ^{14}B , ^{15}B and ^{16}B , using the reactions $^{12}\text{C}(^{14}\text{C},^{12}\text{N})^{14}\text{B}$, $^{13}\text{C}(^{14}\text{C},^{12}\text{N})^{15}\text{B}$ and $^{14}\text{C}(^{14}\text{C},^{12}\text{N})^{16}\text{B}$ at about 24 MeV/A. The mass excess of ^{16}B has been measured for the first time, it is 37.08(6) MeV. This means that ^{16}B is unbound by only 0.04(6) MeV. Furthermore, the nucleus ^{13}B has been investigated with the four reactions $^{16}\text{O}(^{14}\text{C},^{17}\text{F})$, $^{12}\text{C}(^{14}\text{C},^{13}\text{N})$, $^{12}\text{C}(^{13}\text{C},^{12}\text{N})$ and $^{12}\text{C}(^{15}\text{N},^{14}\text{O})$. Choosing different target-projectile combinations, it was possible to populate states with different selectivity. New states are observed in ^{13}B at excitation energies above the threshold for two-neutron decay.

PACS. 21.10.-k Properties of nuclei; nuclear energy levels – 21.10.Dr Binding energies and masses – 25.70.Hi Transfer reactions – 27.20.+n $6 \leq A \leq 19$

1 Introduction

The structure of neutron-rich boron isotopes, which span the neutron numbers $N = 8-14$, has attracted attention over a long time and the position of the dripline at $N = 14$ is now quite well determined. The discovery of the particle stability of ^{14}B and ^{15}B has been reported by Poskanzer et al. [1]. The heaviest observed stable boron isotope is ^{19}B [2]. The stability of ^{17}B has also been proven experimentally [3]. Moreover, the long chain of boron isotopes with 8–14 neutrons gives a good illustration of the pairing effect: the nuclei ^{15}B – ^{17}B – ^{19}B , having 10, 12 and 14 neutrons, are particle stable, while the isotopes ^{16}B and ^{18}B with 11 and 13 neutrons are particle unstable [2–4]. However, until recently very little has been known about the level structure of boron isotopes with $A \geq 14$. Here we report on new results on the structure of the isotopes ^{13}B , ^{14}B , ^{15}B and ^{16}B .

2 Experimental details

We have studied binary reactions using $^{13,14}\text{C}$ and ^{15}N beams from the heavy-ion accelerator at HMI-Berlin. In

^a Permanent address: Institute for Nuclear Research and Nuclear Energy, Bulgarian Academy of Sciences, Blvd. Tsarigradsko Shosse 72, 1784 Sofia, Bulgaria

the multi-nucleon transfer reactions neutron-rich isotopes are reached via multi-step proton pick-up and neutron stripping processes. Here we present results on reactions induced by a ^{14}C -beam on a ^{16}O -target and targets of the carbon isotopes ^{12}C , ^{13}C and ^{14}C , as well as of ^{13}C - and ^{15}N -beams on a ^{12}C -target. The reactions studied are summarized in Table 1. The Q-values are rather negative, thus high incident energies of about 25 MeV/nucleon are needed. The very negative Q-values induce a strong mismatch for reactions with low angular momentum transfer. We therefore do not expect the population of $\ell = 0$ configurations, while in some cases we may have a favoured population of states with high spin and angular momentum ℓ . The ejectiles ^{12}N , ^{13}N and ^{14}O have no excited states, which are stable against particle emission, the measured momentum spectra thus reflect unambiguously the level scheme of the residual nucleus. The ^{17}F ejectile has one particle-stable excited state at $E^* = 0.495$ MeV ($J^\pi = 1/2^+$). However, the analysis has shown that, because of the $\ell = 0$ angular momentum of the neutron of this state, its contribution is strongly suppressed by the dynamics of the reaction.

Measurements have been performed using the Q3D magnetic spectrometer at HMI Berlin. The isotope identification was performed with the focal plane detector by the measurement of the energy loss in the proportional counter, the energy and time-of-flight from the scintillator as described in [6]. The position in the focal plane was

Table 1. Summary of the reactions, projectile energies, energy resolution (δE) and angular openings ($\Delta\Theta_{\text{lab}}$) of the Q3D magnetic spectrometer used in the present work for studying the isotopes ^{13}B , ^{14}B , ^{15}B and ^{16}B . The Q-values for the reactions (1)–(6) are calculated according to [5], the Q-value for reaction (7) is the result of the present work

No.	Isotope	Reaction	Beam energy [MeV]	δE [deg]	$\Delta\Theta_{\text{lab}}$ [MeV]	Q-value [MeV]
(1)	^{13}B	$^{16}\text{O}(^{14}\text{C}, ^{17}\text{F})^{13}\text{B}$	334.4	0.60	1.0–4.3	–20.231(1)
(2)		$^{12}\text{C}(^{14}\text{C}, ^{13}\text{N})^{13}\text{B}$	336.8	0.45	1.4–5.0	–18.888(1)
(3)		$^{12}\text{C}(^{13}\text{C}, ^{12}\text{N})^{13}\text{B}$	336.4	0.30	1.8–5.2	–30.775(1)
(4)		$^{12}\text{C}(^{15}\text{N}, ^{14}\text{O})^{13}\text{B}$	240.1	0.23	2.0–5.4	–24.467(1)
(5)	^{14}B	$^{12}\text{C}(^{14}\text{C}, ^{12}\text{N})^{14}\text{B}$	334.4	0.35	1.1–4.5	–37.982(21)
(6)	^{15}B	$^{13}\text{C}(^{14}\text{C}, ^{12}\text{N})^{15}\text{B}$	337.3	0.40	4.4–6.4	–40.160(22)
(7)	^{16}B	$^{14}\text{C}(^{14}\text{C}, ^{12}\text{N})^{16}\text{B}$	336.6	0.60	2.0–5.0	–48.378(60)

measured by a delay-line read-out. A V_2O_5 -target, 600 $\mu\text{g}/\text{cm}^2$ thick, and ^{12}C -targets, 200 and 500 $\mu\text{g}/\text{cm}^2$ thick, were used. The ^{13}C -target of 300 $\mu\text{g}/\text{cm}^2$ thickness was highly enriched (98%). The ^{14}C -target was 420 $\mu\text{g}/\text{cm}^2$ thick and consisted of ^{14}C (70%), ^{12}C (25%) and ^{16}O (5%). For background subtraction purposes the $(^{14}\text{C}, ^{12}\text{N})$ -reaction was measured also on a ^{12}C - and a V_2O_5 -target. The experimental energy resolutions achieved in the different experiments are also listed in Table 1.

3 Results and discussion

3.1 The isotope ^{13}B

The nucleus ^{13}B has been studied previously in various reactions [7] and many levels up to about 12 MeV excitation energy are already known, as can be seen from Table 2 (first column).

We have populated states in ^{13}B in four different reactions: $^{16}\text{O}(^{14}\text{C}, ^{17}\text{F})$, $^{12}\text{C}(^{14}\text{C}, ^{13}\text{N})$, $^{12}\text{C}(^{13}\text{C}, ^{12}\text{N})$ and $^{12}\text{C}(^{15}\text{N}, ^{14}\text{O})$. We recall that for ^{13}B the neutron and proton numbers are $N = 8$ and $Z = 5$, respectively. Excited states are thus formed by particle-hole excitations across the closed $N = 8$ shell. Choosing different target-projectile combinations, it is possible to populate the final states with different selectivity. We have used two types of reactions:

- (i) a three-proton pick-up from a ^{16}O -target, which populates mainly proton-hole states of ^{13}B due to the pick-up mechanism (reaction (1) in Table 1), and
- (ii) a one-proton pick-up plus two-neutron stripping reaction on ^{12}C , where two neutrons are transferred to the open shells and many neutron-particle states are populated in combination with the one-proton hole (reactions (2)–(4) in Table 1).

The spectra obtained in the four reactions are shown in Figs. 1–4. The energy levels derived from these spectra are the same within the experimental error; they are summarized and compared to the ones known from the literature [7] in Table 2.

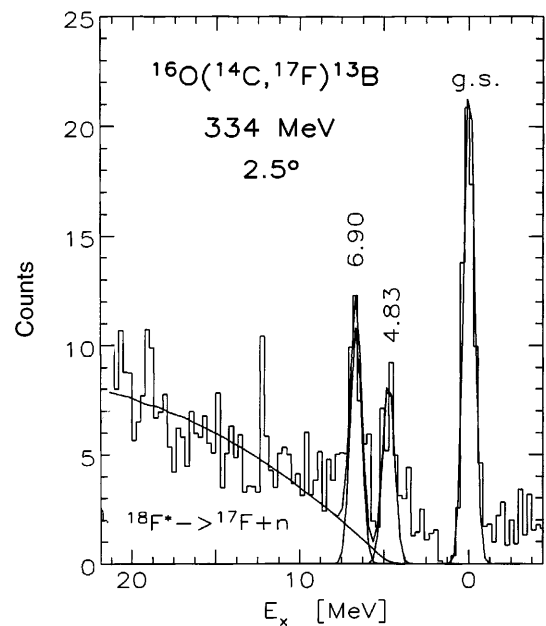


Fig. 1. Excitation energy spectrum for ^{13}B obtained in the reaction $^{16}\text{O}(^{14}\text{C}, ^{17}\text{F})^{13}\text{B}$

3.1.1 The reaction $^{16}\text{O}(^{14}\text{C}, ^{17}\text{F})^{13}\text{B}$

The measurement of the reaction $^{16}\text{O}(^{14}\text{C}, ^{17}\text{F})^{13}\text{B}$ (Fig. 1), which is a three-proton pick-up reaction, was performed at an energy of 334.4 MeV and at the mean angle $\Theta_{\text{lab}} = 2.5^\circ$ (the measured angular range is given in Table 1). As can be seen from the figure, the ground state transition is dominant. Two other transitions, which are 2–3 times weaker, are seen at excitation energies of 4.83 MeV and 6.90 MeV. At higher excitation energies a continuum is observed, which is in general described by a process, where, in a two-body reaction, an excited outgoing particle is formed, which later on decays, e.g. by neutron emission, to the detected particle [8]. Here the reaction $(^{14}\text{C}, ^{18}\text{F}^*)$ is relevant with the sequential decay of highly excited ^{18}F nuclei into $^{17}\text{F} + n$, viz. $^{18}\text{F}^* \rightarrow ^{17}\text{F} + n$. A description of the high energy part of Fig. 1 is obtained with a broad decay-strength distribution having a maximum at $E^*(^{18}\text{F}) = 20$ MeV and a width of 8 MeV.

Table 2. Excited states in ^{13}B populated in four different reactions, their widths Γ [MeV], tentative J^π -assignments and differential cross sections (in the c.m. system; statistical errors are given in brackets). The results are compared to the literature [7]

Ref. [7]	$^{16}\text{O}(^{14}\text{C}, ^{17}\text{F})^{13}\text{B}$		$^{12}\text{C}(^{14}\text{C}, ^{13}\text{N})^{13}\text{B}$		Present work		$^{12}\text{C}(^{15}\text{N}, ^{14}\text{O})^{13}\text{B}$		[MeV]	J^π
	E_x [MeV (keV)]	E_x [MeV]	$d\sigma/d\Omega$ (5.4°) [$\mu\text{b}/\text{sr}$]	E_x [MeV]	$d\sigma/d\Omega$ (5.4°) [$\mu\text{b}/\text{sr}$]	E_x [MeV]	$d\sigma/d\Omega$ (6.2°) [$\mu\text{b}/\text{sr}$]	E_x [MeV]		
0	0	0.28 (3)	0	2.2 (2)	0	1.0 (3)	0	0.3 (1)		$3/2^-$
3.4828 (4.5)										
3.5346 (3.1)										
3.6810 (4.5)										$(5/2^+)$
3.7126 (4.5)			3.68*	5.3 (3)	3.69*	1.8 (4)	3.72*	1.8 (2)		$(5/2^-)$
4.131 (6)			4.13	1.2 (2)	4.12	1.4 (3)	4.14	0.7 (1)		
4.829 (6)	4.83	0.09 (2)	4.91	1.8 (2)						$(1/2^-)$
5.024 (6)					5.00	1.4 (3)	5.03	0.4 (1)		$(3/2^-)$
5.106 (10)										
5.388 (6)			5.39	5.8 (4)	5.37	3.2 (5)	5.38	3.0 (2)		$(7/2^-)$
6.167 (6)							6.17	1.8 (2)	0.06	
6.425 (7)			6.37	15.1 (6)	6.40	19.0 (1.2)	6.43	13.4 (5)	0.03	$(5/2^+ - 9/2^+)$ $(7/2^- - 11/2^-)$
6.934 (9)	6.90	0.10 (2)	6.96	2.0 (2)			6.92	1.2 (2)	0.15	$(3/2^-, 5/2^-)$
(7.516+7.859)			7.58	1.1 (2)	(7.20)	1.9 (4)	7.76	0.5 (1)	0.17	
8.133 (7)			8.14	5.3 (3)	8.16	3.9 (6)	8.12	3.4 (2)	0.07	
8.683 (7)			8.69	1.9 (2)	8.68	3.4 (5)	8.69	2.8 (2)	<0.08	
9.44 (30)			9.44	1.6 (2)	9.31	2.6 (4)	9.44	1.6 (2)	<0.08	
10.22 (20)			10.22	4.0 (3)	10.22	15.1 (1.1)	10.22	9.2 (4)	0.17	$(11/2^-)$
10.89 (20)			10.98	6.4 (4)	11.18	7.1 (7)	11.05	8.0 (4)	0.8–1.2–1.8	
							13.65	1.7 (2)	0.30	
							14.39	1.4 (2)	0.40	

* unresolved two states (3.68 MeV, 3.71 MeV)

The three protons are picked from the even-even ^{16}O -target nucleus, where both the protons and neutrons are coupled to spin zero. The neutrons are not involved in the reaction - in first order their configuration is assumed to stay unchanged. Thus, the reaction populates selectively proton-hole states of the residual nucleus. One should therefore expect that, since the three outermost protons are removed, the $\pi 1p3/2$ -ground-state configuration is strongly preferred in this reaction. As can be seen from Fig. 1, this is indeed the case. The excited state at 4.83 MeV can be the result of the pick-up of one proton from the $1p1/2$ -shell, and of two protons from the $1p3/2$ -shell leaving the other two protons coupled to spin 0^+ . This would allow a possible $1/2^-$ -assignment for the 4.83 MeV state. The 6.90 MeV state can be formed by the same $1/2^-$ -configuration with the two protons left in the $p3/2$ -shell, but coupled to 2^+ , giving possible values of $J^\pi = 3/2^-$ and $5/2^-$. It is worth noting that in shell-model calculations of Millener and Kurath [9], using the Cohen-Kurath interaction, levels at 4.60 and 6.69 MeV have been obtained with spins $1/2^-$ and $5/2^-$, respectively. Thus similarly to the conclusions of [10], we see that in order to explain the experimental spectrum, it is not necessary to involve the ^{16}O -target-nucleus ground state configuration mixing obtained in a calculation of Wolters et al. [11].

An additional excitation of strong collective neutron configurations, with spin of 2^- or 3^- , may also be pos-

sible by the promotion of a $1p1/2$ neutron to the $1d5/2$ -shell. However, as such excitations require one more step in the reaction process, we expect that they have a negligible cross section as compared to the direct three-proton transfer.

3.1.2 The reactions $^{12}\text{C}(^{14}\text{C}, ^{13}\text{N})^{13}\text{B}$, $^{12}\text{C}(^{13}\text{C}, ^{12}\text{N})^{13}\text{B}$ and $^{12}\text{C}(^{15}\text{N}, ^{14}\text{O})^{13}\text{B}$

These reactions also involve a three-nucleon transfer. Here, one proton is picked up from the target and two neutrons are transferred to the target, so at least two transfer steps are necessary and either of these could be the first one. In all reactions a ^{12}C -target has been used. We show the spectra in Figs. 2, 4, 5. We see that the neutron transfer into open shells populates many excited states of ^{13}B . However, the excited states at about 4.8 and 6.9 MeV, observed in the three-proton pick-up reaction, are seen as very weak peaks only. Also, the ground state is comparatively weakly populated.

The reaction $^{12}\text{C}(^{14}\text{C}, ^{13}\text{N})^{13}\text{B}$. Let us first consider the $^{12}\text{C}(^{14}\text{C}, ^{13}\text{N})^{13}\text{B}$ reaction. The spectrum obtained is shown in Fig. 2. The background is completely explained by a three-body channel corresponding to the sequential

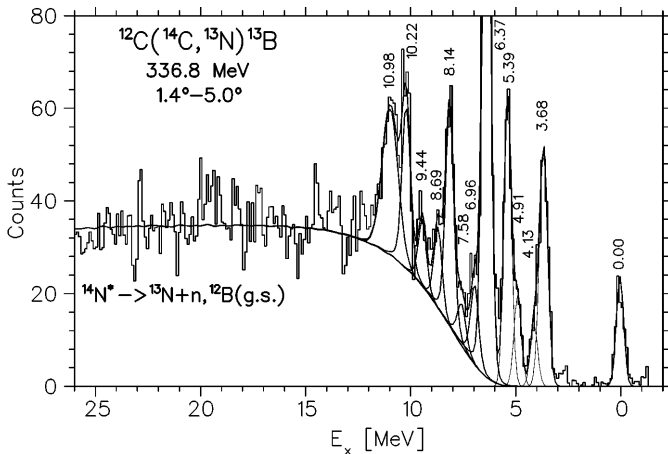


Fig. 2. Excitation energy spectrum for ^{13}B obtained in the $^{12}\text{C}(^{14}\text{C}, ^{13}\text{N})^{13}\text{B}$ reaction

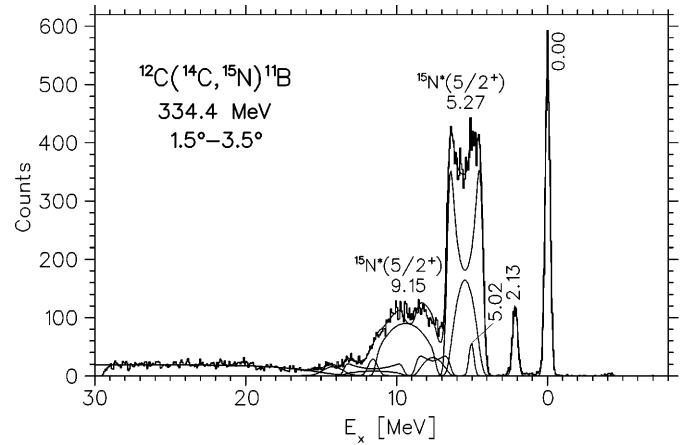
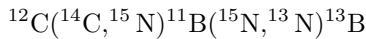


Fig. 3. Excitation energy spectrum for ^{11}B obtained in the reaction $^{12}\text{C}(^{14}\text{C}, ^{15}\text{N})^{11}\text{B}$ at 334.4 MeV and 2.5° [6]. The fit has been done using the method of [8]

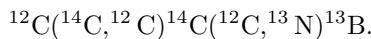
decay in-flight of a highly excited $^{14}\text{N}^*$ nucleus into $^{13}\text{N} + n$. The residual nucleus ^{12}B in this case is produced predominantly in its ground state.

The transfer of three nucleons can also be considered as taking place in two steps, i.e. we can describe the reaction as a sequential mechanism with the pick-up of a proton and the transfer of two neutrons, which are treated as a single-cluster entity (because they both originate from the $p1/2$ -shell). It is supposed that the sequential transfer of single nucleons, which is of higher order, gives much smaller contributions. As the most probable we can discuss the following cases, depending on the choice of the first step:

(Ai) Pick-up of one proton from the ^{12}C -target and stripping of two neutrons:



(Aii) Stripping of two neutrons from the projectile and pick-up of one proton:



In case (Ai), the first step is a one-proton pick-up reaction on ^{12}C , leading to ^{11}B as the residual nucleus. The pick-up of the proton occurs most probably from the $\pi p3/2$ -target-shell and also from the $p1/2$ -shell (taking into account the ground state configuration mixing of ^{12}C). The reaction $^{12}\text{C}(^{14}\text{C}, ^{15}\text{N})^{11}\text{B}$ has been used for another purpose [6] and it has been found that the ground state ($J^\pi = 3/2^-$) of ^{11}B is populated very strongly, as one could expect for a proton pick-up reaction (Fig. 3). The first excited state (2.13 MeV, $1/2^-$) of ^{11}B is also populated, but with smaller intensity. In the second step, the two neutrons stripped from ^{15}N can be transferred to any unoccupied shell of the ^{11}B -core. As a result, many different spin couplings are possible. The two neutrons can be placed on the ^{11}B nucleus into $p1/2$, $s1/2$, $d5/2$ orbits forming predominantly $2n$ -configurations of natural parity such as 0^+ , 1^- , 2^+ , 3^- or 4^+ , which are coupled to the $p3/2$ -proton, and as many as about 10 J^π -values can occur

for the excited states of ^{13}B , giving more states than are visible in the experimental spectrum. The transfer of the two neutrons into the $1d5/2$ -shell is strongly favoured by the reaction mechanism. The strongly populated state at 6.37 MeV might be due to the highest spins (3^- or 4^+) of neutron states coupled to the $p3/2$ -proton. This state thus would have the highest spin in the range of $5/2^+ - 9/2^+$ or $7/2^- - 11/2^-$.

Comparing the structure of ^{11}B and ^{13}B , we can assume that the lowest lying states are obtained by coupling of the $p3/2$ proton to the lowest lying 2^+ (neutron) excitation. Thus in ^{11}B a multiplet is formed with spin values $1/2^-, 3/2^-, 5/2^-, 7/2^-$; the $3/2^-$ is pushed up due to its interaction with the $p3/2$ ground state. For ^{13}B the corresponding multiplet is formed by $^{12}\text{Be}(2^+) \otimes \pi p3/2$ with the same ordering of spins. The yield in the present experiment of these states follows approximately the expected proportionality $\sigma_J \sim (2J+1)$, if the two $3/2$ -states are taken together.

The same arguments apply to case (Aii), where in the first step two neutrons from the ^{14}C -projectile are transferred to the ^{12}C -target nucleus either to the $1p1/2$ -subshell or to the sd -shell. The mechanism of the reaction again favours in two-nucleon transfer the states of natural parity, with $J^\pi = 3^-, 4^+$ in ^{14}C , because they involve $d5/2$ -orbits, viz. $(1d5/2)^2$ and $[(1p1/2)^1 \otimes (1d5/2)^1]$, [12]. This supposition is confirmed by Fig. 6, where the two-neutron transfer reaction $^{12}\text{C}(^{14}\text{N}, ^{12}\text{N})^{14}\text{C}$ is demonstrated to populate most strongly the 3^- and 4^+ states in the residual ^{14}C nucleus. The more weakly populated states can be formed by other couplings to lower spins. The second step of the reaction involves the removal of one proton from the target. This means that the ^{13}B levels thus are determined by the coupling of the $p3/2$ -proton-hole with the possible neutron configurations of the first step. In particular, we can expect that the strong peak at 6.37 MeV belongs to a high spin state of a multiplet obtained by coupling the $p3/2$ -proton-hole with the 3^- or 4^- states in ^{14}C .

Let us again consider the states at 4.91 MeV and 6.96 MeV, which are more weakly populated. They can be formed in different ways with higher order processes, as was discussed earlier. These ways of reaching the states at 4.91 and 6.96 MeV need 2nd-order proton excitations, this will be an explanation of their weaker population in this reaction compared to the three-proton pick-up $^{16}\text{O}(^{14}\text{C}, ^{17}\text{F})^{13}\text{B}$ reaction of Sect. 3.1.1.

Other mechanisms of forming ^{13}B states are also possible. For instance, we can take as a first step the reaction $^{12}\text{C}(^{14}\text{C}, ^{13}\text{C})^{13}\text{C}$, in which the neutron is stripped on the ^{12}C -target nucleus so that ^{13}C is formed in its ground state ($J^\pi = 1/2^-$) or in any of its single particle excited states (e.g. with $J^\pi = 1/2^+$, $5/2^+$, $3/2^+$). Experimentally this is an analog to the $^{12}\text{C}(^{12}\text{C}, ^{11}\text{C})^{13}\text{C}$ -reaction in which, as has been shown [12], the ground state, the 3.85 MeV ($5/2^+$) and the 7.68 MeV ($3/2^+$) states of ^{13}C are predominantly populated, while the 3.09 MeV ($1/2^+$) state is relatively weakly populated. Starting from such configurations in ^{13}C we can consider going to ^{13}B by first removing one p3/2-proton and adding a neutron to the 1p1/2-shell (or reversing these two steps) coming finally to the same configurations discussed earlier.

Conclusions made in [13] and calculations of [14] propose two doublets of $J^\pi = 3/2^+$, $5/2^+$ at about 3.5 MeV and 7.0 MeV assigned as spin-dipole transitions. Here it should be noted that our energy resolution does not allow distinguishing which of the two states, 3.68 or 3.71 MeV (or both in some ratio), are populated in the studied reaction. However, according to [15] for these closely spaced levels the same spin value is possible. In [16] a value of $J^\pi = 5/2^-$ is deduced for the 3.71 MeV state, and $J^\pi = 5/2^+$ for the 3.68 MeV state. In our measurement the strength of the peak at about 3.7 MeV indicates that the two neutrons are most probably transferred into the 1d5/2-shell. In this case the population of the negative parity state ($5/2^-$, 3.71 MeV) is expected due to the coupling $\nu(d5/2)^2 \otimes \pi 3/2^-$.

The reaction $^{12}\text{C}(^{13}\text{C}, ^{12}\text{N})^{13}\text{B}$. The ^{12}N -spectrum from the $^{12}\text{C}(^{13}\text{C}, ^{12}\text{N})^{13}\text{B}$ reaction, shown in Fig. 4, can be discussed in a similar way as that of the $(^{14}\text{C}, ^{13}\text{N})$ reaction. However, we notice that in this case the Q-value is more negative and that in addition to the state at $E^* = 6.40$ MeV, the 10.22 MeV state is more strongly populated. The states at $E^* = 8.16$, 8.68 and 9.31 MeV are populated with practically equal strength, whereas in the $(^{14}\text{C}, ^{13}\text{N})$ reaction the state at $E^* = 8.14$ prevails. It is noticeable that these states have very small widths (see Table 2). Next to the 10.22 MeV peak we observe a broad structure at about 11.1 MeV, which may be associated with several unresolved peaks, however the statistics and the energy resolution do not allow to draw any definite conclusion.

The background at higher excitation energies is described by the sequential decay of excited $^{13}\text{N}^*$ -ejectiles, formed in the single-charge-exchange reaction $^{12}\text{C}(^{13}\text{C}, ^{13}\text{N})^{12}\text{B}$ and which further decay to ^{12}N by the emission of one neutron. It is known [17] that in this case most strongly populated in the residual ^{12}B nucleus are

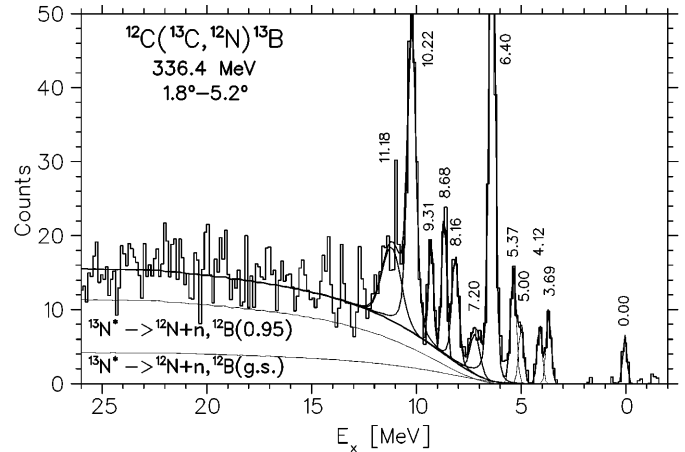
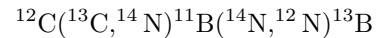


Fig. 4. Excitation energy spectrum for ^{13}B obtained in the $^{12}\text{C}(^{13}\text{C}, ^{12}\text{N})^{13}\text{B}$ reaction

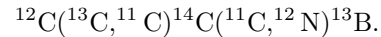
the first excited state at 0.95 MeV (2^+) and the ground state (1^+). It can be seen from Fig. 4 that the superposition of these two amplitudes in the ratio of 1:2.8 gives a satisfactory description of the background.

As most probable we consider the following mechanisms of exchanging the three nucleons:

(Bi) Pick-up of one proton from ^{12}C and stripping of two neutrons:



(Bii) Stripping of two neutrons from the projectile and pick-up of one proton:



Case (Bi) involves the pick-up of one proton from ^{12}C producing ^{11}B as a residual nucleus, the ground state of which is predominantly populated. The second step is a two-neutron transfer on ^{11}B . In principle, the same arguments as in (Ai) can be used. However, in the present case the two neutrons come from different subshells of ^{14}N with different spin coupling ($p1/2$ and $p3/2$). This enforces a larger spin transfer, $\Delta S = 2$, and thus a larger angular momentum transfer than in the previous case with the ^{14}C beam (case (Ai)). The high spin values of the two-neutron configurations are thus enhanced, which can explain the stronger population of the 8.68 and 9.31 MeV states, and especially of the 10.22 MeV state (this feature is supported by the more negative Q-value).

The same argument applies to case (Bii), which represents the reversed order for the transfer steps of (Bi). The first step of (Bii), viz. $^{12}\text{C}(^{13}\text{C}, ^{11}\text{C})^{14}\text{C}$, involves the transfer of two neutrons from ^{13}C to ^{12}C (as mentioned before, neutrons from the 1p1/2 and 1p3/2 shells). The transferred neutrons are allowed to occupy any orbit above the ^{12}C -core starting from the 1p3/2-subshell, due to the configuration mixing in the ground state of ^{12}C . In the second step, one proton is taken away from these states in ^{14}C , the neutron configuration being left intact, thus the first step predetermines the population of states in ^{13}B .

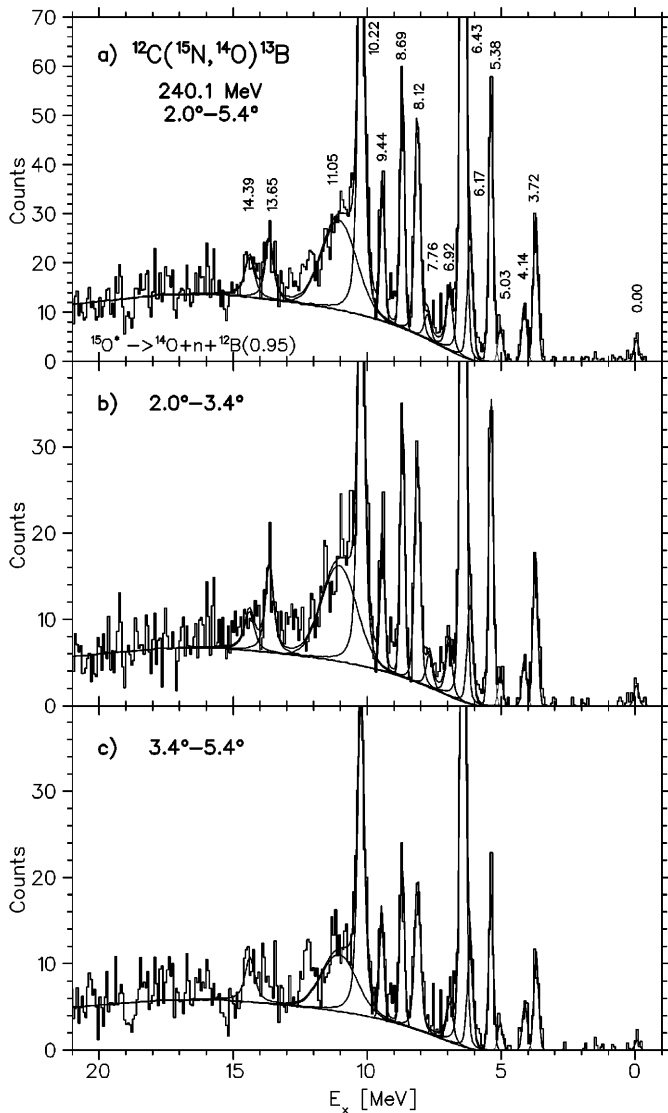


Fig. 5. Excitation energy spectra for ^{13}B obtained in the reaction $^{12}\text{C}(^{15}\text{N}, ^{14}\text{O})^{13}\text{B}$: a) in the full measured angular range, b) at $2.0^\circ < \Theta_{\text{lab}} < 3.4^\circ$ and c) at $3.4^\circ < \Theta_{\text{lab}} < 5.4^\circ$

The strong peaks at 6.40 MeV and 10.22 MeV would be formed by coupling of the $1p_{3/2}$ proton-hole with the 3^- and 4^+ states in ^{14}C . (We have already demonstrated in Fig. 6, that the 3^- and 4^+ states in ^{14}C are most strongly populated).

The reaction $^{12}\text{C}(^{15}\text{N}, ^{14}\text{O})^{13}\text{B}$. The excitation energy spectra of ^{13}B , obtained in this reaction, are shown in Fig. 5 for the full angular range measured (upper panel), two different angular cuts are also shown in addition. Among the four measured reactions for ^{13}B , this one has the best energy resolution (230 keV) and also a relatively lower background, obtained with ^{14}O as an ejectile.

The ground state is seen in all cases, but it is much weaker than in the $^{12}\text{C}(^{14}\text{C}, ^{13}\text{N})^{13}\text{B}$ and $^{12}\text{C}(^{13}\text{C}, ^{12}\text{N})^{13}\text{B}$ reactions. However, the strong similarity with the

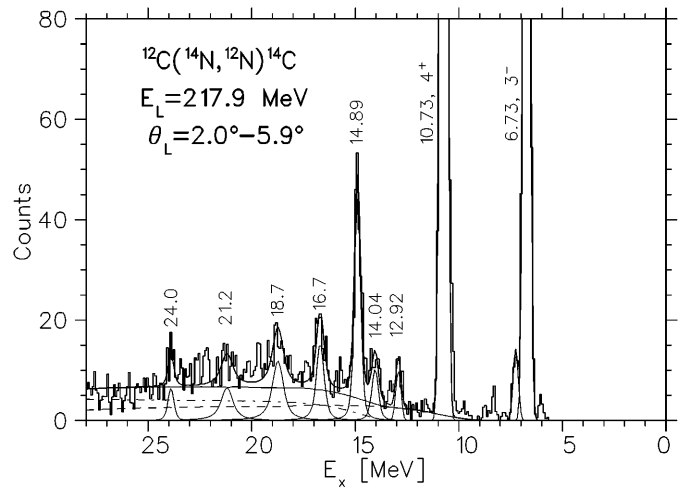
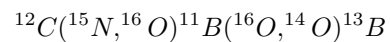


Fig. 6. Excitation energy spectrum obtained in the $^{12}\text{C}(^{14}\text{N}, ^{12}\text{N})^{14}\text{C}$ reaction. States below 6.73 MeV excitation energy were not in the accepted range of momenta in the focal plane

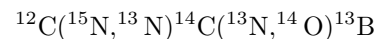
$^{12}\text{C}(^{13}\text{C}, ^{12}\text{N})^{13}\text{B}$ reaction is obvious, the states at 6.43 and 10.22 MeV being most strongly populated, also similar shapes in the excitation energy range $8 \div 13$ MeV are observed. Again a broad structure at about $E^* = 11$ MeV is seen (it may be associated with several unresolved peaks); because of the fluctuations, we have used a broad Gaussian shape of 1.8 MeV width to describe it. New states are observed for the first time at excitation energies $E^* \sim 14$ MeV, which is above the threshold for $2n$ -decay (8.248 MeV [7]). As can be seen from the changing height of the peaks (Fig. 5b and c), these states have different angular distributions, which allows to determine their excitation energy. The background in this case can again be explained involving sequential decay with ^{12}B as the partner of the ^{15}O excited nucleus formed in the first stage of the reaction and decaying in-flight.

This reaction, as the previous ones, involves the exchange of three nucleons and can be described in a similar way:

(Ci) Pick-up of one proton from ^{12}C and stripping of two neutrons:



(Cii) Stripping of two neutrons from the projectile and pick-up of one proton:



Cases (Ci) and (Cii) are similar to (Ai,Aii) and (Bi,Bii). The intermediate ^{11}B and ^{14}C nuclei are formed, followed by placing two neutrons on the first one or stripping a proton from the second one, to get ^{13}B as a residual nucleus. Here, as in cases (Bi) and (Bii), there is a tendency for populating high-spin states based on the coupling of the $p_{3/2}$ -proton-hole with the 3^- and 4^+ states in ^{14}C .

Finally, the following results concerning the strong population of some states in ^{13}B can be collected. The strongest excited states of ^{13}B can be formed by the pick-up of one proton from an excited $^{14}\text{C}^*$ nucleus in the 3^- or 4^+ states. These states have the neutron configurations $[\nu p1/2 \otimes \nu d5/2]$ and $[\nu d5/2]^2$, which then couple with the $p3/2$ -proton-hole in ^{13}B . For this reason the most strongly populated states at 6.43 MeV and 10.22 MeV are predicted to have most probably $J^\pi = 9/2^+$ and $11/2^-$. We could also consider ^{12}B as a core on which one neutron is added to produce ^{13}B . In such a case we come to the same conclusions. As has been observed in charge exchange reactions [17,18], the most prominent peak observed in ^{12}B at about 4.5 MeV has $J^\pi = 4^-$ (this peak contains also a strong 2^- state). In [18] it has been concluded that the structure at 4.5 MeV in the spectrum of ^{12}B may correspond to the state at about 6.3 MeV in ^{13}B . Thus starting from this 4^- state in ^{12}B and placing a neutron on the $p1/2$ -shell to form ^{13}B , we get for the 6.43 MeV state a possible spin assignment $9/2^+$. Starting with the same 4^- state and placing a neutron on the $d5/2$ -shell we would get the next higher most strongly populated state with $J^\pi = 11/2^-$ at 10.22 MeV.

3.2 The isotope ^{14}B

The nucleus ^{14}B has been controversially predicted to be particle unstable by Ball et al. [19], whereas Garvey and Kelson [20] predicted it to be particle stable by about 400 keV. An experiment, using the spallation reaction $\text{U} + \text{p}$ (5.3 GeV) to produce isotopes of light elements, proved that ^{14}B is particle stable [1].

The mass excess of ^{14}B has been determined for the first time by Ball et al. using the reaction $^{14}\text{C}(^7\text{Li}, ^7\text{Be})^{14}\text{B}$ as 23.657 ± 0.030 MeV [21]. Practically the same value (M.E. = 23.67 ± 0.30 MeV) was obtained in the reaction $^{14}\text{C}(^{14}\text{C}, ^{14}\text{N})^{14}\text{B}$ at 87.4 MeV in [22]. Averaging these two values, it follows that ^{14}B is stable with respect to the decay into $^{13}\text{B} + \text{n}$ by about 0.97 MeV [5], i.e. it is more strongly bound than predicted in [19,20]. Shell-model calculations [23] give 0.986 MeV in good agreement with the experimental value for the stability of ^{14}B . In [21] five excited levels, all below 3 MeV excitation energy, are observed: 0.74(4) MeV, (1^-); 1.38(2) MeV, (3^-); 1.82(6) MeV, (2^-); 2.08(5) MeV, (4^-); and 2.97(4) MeV. The shown spins and parities have been assigned according to the similarity of the spectra for $^{14}\text{B}^*$ and $^{12}\text{B}^*$ (measured in the same experiment). The three observed states above the neutron threshold (0.97 MeV) have a width less than 0.3 MeV. The strongest among these levels is the state at $E^* = 2.08$ MeV ($J^\pi = 4^-$), but the spectrum is rather complicated because of the doublet of particle stable states in ^7Be ($3/2^-$ -ground state and $1/2^-$ -first excited state at 0.429 MeV).

The reaction $^{14}\text{C}(\pi^-, \gamma)^{14}\text{B}$ [24] has led to the observation of one strong transition at $E^* = 2.15 \pm 0.17$ MeV, which has a width of 1.0 ± 0.5 MeV. In contrast to the ($^7\text{Li}, ^7\text{Be}$)-reaction where higher-spin states can be populated, the transitions in the (π^-, γ) -reaction do not involve

large angular momentum transfers, and the population of a 4^- state is expected to be weak. For this reason, the strong and broad state at 2.15 MeV was assigned by Baer et al. [24] as 2^- . This seems to be on the first sight controversial to the observations of Ball et al. [21], where the 2^- state is reported at 1.82 ± 0.06 MeV, but the latter state is observed as part of a broader structure, which was not analyzed with the correct line shape of Breit-Wigner resonances. As suggested in [24] a consistent picture for this region of excitation is obtained with a narrow 4^- state and a broad 2^- resonance both centered at about 2.1 ± 0.1 MeV. In the $^{14}\text{C}(\pi^-, \gamma)^{14}\text{B}$ reaction indications for higher lying transition strength with $J^\pi = 2^-$ or 1^- were found: a very broad structure centered at about 6.7 ± 1.6 MeV with a width of 7.8 ± 3.2 MeV. No distinct peak could be separated in the very complex experimental spectrum. Quite recently, in the study of the β -delayed neutron decay of ^{14}Be , a strong neutron group was observed leading to a final state in ^{14}B at 1.28 ± 0.02 MeV excitation energy having a width of 60 keV, and a tentative spin-parity assignment $J^\pi = 1^+$ has been made [25]. Another 1^+ level was also observed by Belbot et al. at 4.31 MeV.

We have investigated the structure of ^{14}B by the reaction $^{12}\text{C}(^{14}\text{C}, ^{12}\text{N})^{14}\text{B}$ at a beam energy of 334.4 MeV and for an angular range of $1.1^\circ < \Theta_{\text{lab}} < 4.5^\circ$. Figure 10a shows the measured ^{12}N -spectrum. The energy resolution in the experiment was 350 keV. The ground state of ^{14}B is very weakly populated. So are the other low-lying states below 2 MeV excitation energy. The next strongest peak is observed at $E^* = 2.08$ MeV, a situation similar to the ($^7\text{Li}, ^7\text{Be}$) reaction in [21]. The width of the line corresponds to the experimental resolution (0.35 MeV), therefore only an upper limit of 0.1 MeV can be estimated for the total width of this resonance. From the small width we conclude that this line corresponds to the excitation of the 4^- state, and the broader counting rate distribution below may represent the broader 2^- resonance (the same conclusion was drawn by Bear et al. [24]). A similar situation is met for the isotope ^{12}B , where the 4^- and 2^- states are located closely together at $E^* = 4.52$ MeV and 4.46 MeV, respectively, with widths of 0.11 MeV and about 0.30 MeV [7].

The weak population of the ground state is explained by the reaction mechanism, which favours large angular momentum transfers. The dominant configurations of the 2^- ground state and 1^- first excited state at 0.74 MeV are given by the couplings $(\pi 1p3/2 \otimes \nu 2s1/2)$ to 2^- and 1^- , respectively, (see, e.g., [24]). The $2s1/2$ neutron orbit causes the weak population in our reaction. In contrast to this, the population of the $4^-/2^-$ doublet at about $E^* = 2.1$ MeV is more favoured, because both states are based on the configuration $(\pi 1p3/2 \otimes \nu 1d5/2)$.

We observe furthermore strong peaks lying above the threshold for two-neutron emission ($S_{2n} = 5.848$ MeV) at excitation energies of 6.96 MeV, 8.03 MeV and 10.15 MeV. The data show also indications for the existence of states at excitation energies of about 4.5 and 6.0 MeV. The structure at about 6 MeV excitation energy may consist of more than one peak. Some of the observed peaks are ob-

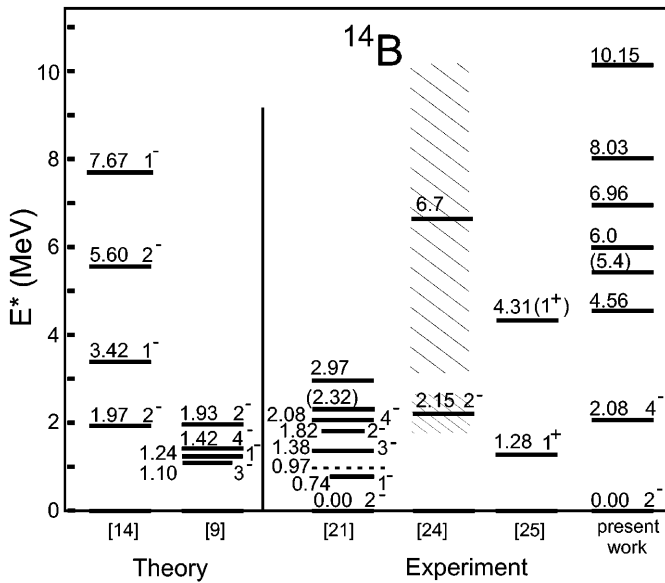


Fig. 7. Comparison of theoretical predictions on the ^{14}B -nucleus from [9,14] with experimental results from [21,24,25] and the present work. The dashed line denotes the energy threshold for one-neutron emission. The hatched areas indicate the width (FWHM) of broad resonances

served on a rising continuum. The latter can be attributed to a three-body background resulting from the decay in-flight of highly excited $^{13}\text{N}^*$ nuclei into $^{12}\text{N} + n$, and to a four-body continuum coming from the decay in-flight of $^{14}\text{N}^*$ into $^{12}\text{N} + 2n$. The shapes of the respective contributions are quite different. The three-body background is relatively low due to the three-nucleon transfer leading to population of the decaying $^{13}\text{N}^*$. The contribution of the $^{14}\text{N}^*$ -decay is much stronger.

Figure 7 displays the present knowledge, theoretical (left side) and experimental (right side), on ^{14}B . In [9], the spectrum of ^{14}B has been calculated using different particle-hole interactions, one example is presented – it covers excitation energies of only up to ~ 2 MeV, the spin assignments being reversed to the ones deduced experimentally [21]. We distinctly see the level at 4.56 MeV, which is close to the value of 4.31 MeV observed in [25]. While a broad bump has been observed at $E^* \approx 6$ MeV in [24], in our spectrum there are indications of 3 peaks between 5 and 7 MeV excitation energy, which can be also connected to the values predicted in the same range by the shell-model calculations in [14]. Table 3 summarizes the result (excitation energies, cross sections and significance) for the levels of ^{14}B observed in the present work.

3.3 The isotope ^{15}B

The nucleus ^{15}B has been established to be particle stable with respect to one-neutron emission by 2.77 MeV [26,27]. However, no experimental data is available on its excited states. Theoretically the structure of ^{15}B has been studied extensively using shell-model calculations [23,28], as well as antisymmetrized molecular dynamics [29].

Table 3. Excitation energies, widths and differential cross sections at $\theta_{\text{cm}} = 5.4^\circ$ for excited states of ^{14}B populated in the $^{12}\text{C}(^{14}\text{C}, ^{12}\text{N})^{14}\text{B}$ reaction

E_x (J^π) [MeV]	Γ [MeV]	$d\sigma/d\Omega$ (5.4°) [nb/sr]
g.s. (2^-)		
2.08 ($4^- + 2^-$)		76 (13)
4.56(5)		42 (10)
(5.4)		41 (10)
5.95(8)		72 (13)
(6.2)		41 (10)
6.96(5)		157 (19)
8.03(5)	0.60	350 (28)
(8.86)	0.20	45 (10)
10.15(9)	0.60	204 (22)

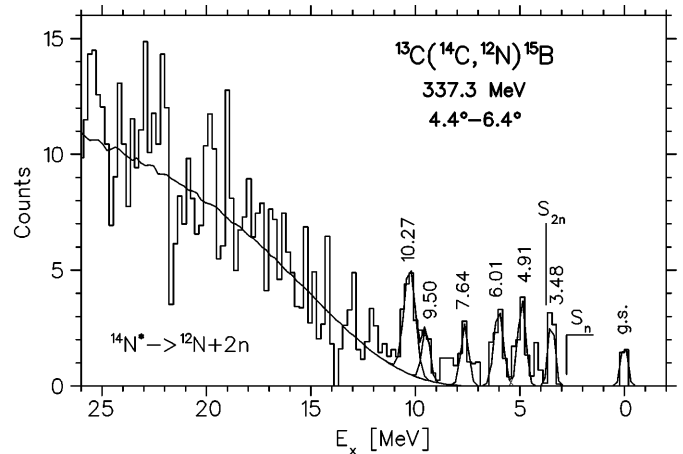


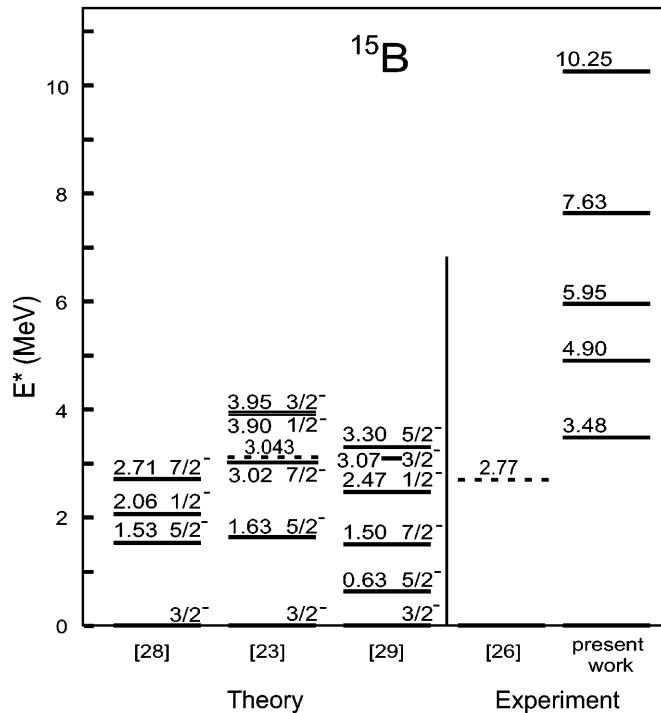
Fig. 8. Excitation energy spectrum of the $^{13}\text{C}(^{14}\text{C}, ^{12}\text{N})^{15}\text{B}$ reaction

We have studied the nucleus ^{15}B in the reaction $^{13}\text{C}(^{14}\text{C}, ^{12}\text{N})^{15}\text{B}$ at a beam energy of 337.3 MeV. Figure 8 shows the ^{12}N -spectrum, obtained in the angular range $4.4^\circ < \Theta_{\text{lab}} < 6.4^\circ$. The energy resolution in this case was 400 keV. In addition to the ground state, in spite of the rather low statistics, but with no background, one can distinguish a few lines corresponding to formerly unknown states in ^{15}B at $E^* = 3.48, 4.91, 6.01, 7.64, 9.50$ and 10.27 MeV. In this case the three-body background from the $^{13}\text{N}^*$ decay is again very low due to the complicated three-nucleon transfer to produce the excited $^{13}\text{N}^*$. This allows to accept the peaks between 4.90 MeV and 7.63 MeV as states belonging to ^{15}B , since this region is still almost background free. The high-energy background (above ~ 8 MeV) results from the sequential decay of ^{14}N in the exit channel: $^{14}\text{N}^* \rightarrow ^{12}\text{N} + 2n$.

Figure 9 presents the different theoretical predictions for excited states in ^{15}B and compares them with our experimental results, which are given in Table 4. There is an obvious discrepancy between the experimental level energies and the theoretical predictions: no state is observed below 3.4 MeV experimentally, whereas most of the theoretically calculated levels are falling below 3.5 MeV. This

Table 4. Excitation energies and differential cross sections in the c.m. system at $\theta_{\text{cm}} = 11.3^\circ$ (statistical errors in brackets) for the states of ^{15}B , observed in the $^{13}\text{C}(^{14}\text{C}, ^{12}\text{N})^{15}\text{B}$ reaction

E_x [MeV]	g.s.	3.48(6)	4.90(6)	6.00(8)	7.64(8)	9.50(10)	10.27(8)
$d\sigma/d\Omega$ (11.3°) [nb/sr]	18 (10)	28 (12)	44 (15)	46 (16)	31 (13)	26 (12)	81 (21)

**Fig. 9.** Energy levels of ^{15}B obtained in the present experiment, compared to different theoretical predictions [23,28,29]. The dashed line denotes the energy threshold for one-neutron emission

discrepancy seems not to be surprising, if one recalls the level scheme of ^{13}B and compares it to that of ^{15}B . In ^{13}B the first excited state also lies at $E^* > 3$ MeV. In [27] considerations are given also favouring the absence of low-lying states in ^{15}B with $E^* < 2$ MeV.

3.4 The isotope ^{16}B

It has been proven by the measurements of Bowman et al. [3] and Langevin et al. [4] that the nucleus ^{16}B is certainly particle unstable. That it is unbound with respect to the decay into $^{15}\text{B} + n$ has been predicted in [20]: the threshold is predicted at $S_n = -1.0 \pm 0.4$ MeV. The instability of ^{16}B is confirmed by shell-model calculations [23], though it is predicted to be significantly less unbound ($S_n = -0.164$ MeV). Shell-model calculations [23,28] predict excited states in ^{16}B as well. The ^{16}B -levels are of great interest for calculations of the structure of ^{17}B , whose ground state is a candidate for a neutron halo structure [30].

In the present work the mass of ^{16}B has been measured for the first time, using the $^{14}\text{C}(^{14}\text{C}, ^{12}\text{N})^{16}\text{B}$ reac-

tion at 336.6 MeV (Fig. 10b) with an energy resolution of about 600 keV; a short summary of this result was given in [31]. The measured ^{12}N -energy spectrum shows besides the reaction on ^{14}C also the $(^{14}\text{C}, ^{12}\text{N})$ reaction on the ^{12}C -content (25%) in the target. The three strong ^{14}B -peaks at $E^* = 6.96$ MeV, 8.03 MeV and 10.15 MeV, discussed before (Fig. 10a), have been clearly identified on the right-hand side of Fig. 10b as indicated. These lines have been used for the energy calibration of the mass excess. The fit to the spectrum was obtained by using a $^{12}\text{C}(^{14}\text{C}, ^{12}\text{N})^{14}\text{B}$ -spectrum measured independently on a ^{12}C -target, shown by the thick line in Fig. 10b, which is scaled to the ^{14}B -peaks observed on the right.

Between the two ^{14}B -states at 8.03 MeV and 10.15 MeV the lowest-lying ^{16}B peak can be identified (see Fig. 10b). It is found at a position which corresponds to a value of $Q_0 = -48.38(6)$ MeV. Thus, a mass excess of 37.08(6) MeV can be determined for this ^{16}B -peak. It means that this state is unbound by only 40 keV with respect to the neutron-decay and the error of the Q -value even overlaps the neutron threshold. Since ^{16}B is definitely neutron unstable, the error bars allow only a peak position between the neutron threshold and 0.1 MeV above it. Since it is rather unprobable, although possible, that there is another ^{16}B -state in the 40 keV range between the observed peak and the neutron threshold, we tentatively assign this peak as the ground state of ^{16}B . For the width of this resonance only an upper limit can be given: $\Gamma < 100$ keV. Two other resonances of ^{16}B are distinguished: at $E^* = 2.36(7)$ MeV and tentatively at 6.06(8) MeV. The latter is uncertain because of the large statistical fluctuations observed in this region. In the lower panel of Fig. 10 the spectrum of ^{16}B -states is shown after subtraction of a normalized spectrum of the $^{12}\text{C}(^{14}\text{C}, ^{12}\text{N})^{14}\text{B}$ reaction, and in Table 5 the information on ^{16}B is summarized (excitation energies, resonance energies above the particle threshold, widths, differential cross sections and significances).

If we adopt the shell-model picture, the last odd proton and the last odd neutron in ^{16}B occupy the $1p_{3/2}$ and the $1d_{5/2}$ orbitals, respectively. These two nucleons can couple to $J^\pi = 1^-, 2^-, 3^-$ and 4^- . According to the weak Nordheim rule, for ^{16}B , which is an odd-odd nucleus with both odd nucleons having ℓ and s parallel, most probable values for the spin and parity of the ground state are $J^\pi = 4^-$ or 3^- . The reaction used is expected to populate strongly unnatural parity states similar to the $(^{12}\text{C}, ^{12}\text{N}_{1+})$ reaction [17]; thus we expect the 4^- -state to be the strongest and the 3^- and 1^- states to be weak. A comparison can be made for excitation energy spectra of ^{16}B and ^{14}B . As we have seen for the case of ^{14}B (Fig. 10a), the 4^- -state at $E^* = 2.08$ MeV with the corresponding

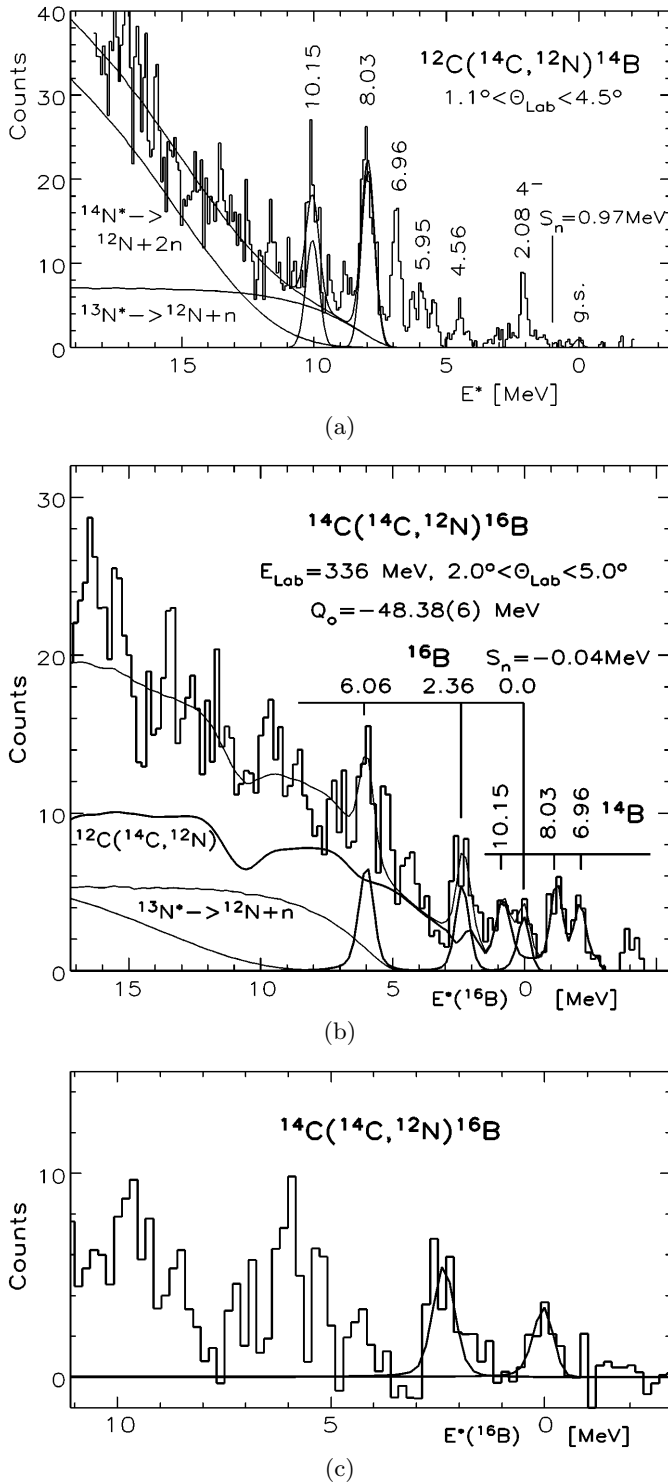


Fig. 10. Excitation energy spectra (a) of the $^{12}\text{C}(^{14}\text{C}, ^{12}\text{N})^{14}\text{B}$ reaction (upper panel) – this spectrum also illustrates the determination of the background in spectrum (b) for ^{16}B – and (b) of the $^{14}\text{C}(^{14}\text{C}, ^{12}\text{N})^{16}\text{B}$ reaction (center panel). The spectra are shown in such a way that the 4^- state in ^{14}B is aligned with the ground state of ^{16}B . The full curves show the results of three body decay strength and of the background due to the ^{12}C -content in the ^{14}C -target. The lower panel (c) shows the ^{16}B spectrum on an expanded scale after subtraction of the background from the ^{12}C -content in the target

Table 5. Excitation energies, energies above the neutron threshold (resonance energies E_R), widths, significance and cross sections in the c.m. system at $\theta_{\text{cm}} = 5.1^\circ$ (statistical errors in brackets) for states of ^{16}B , observed in the $^{14}\text{C}(^{14}\text{C}, ^{12}\text{N})^{16}\text{B}$ reaction. The statistical significance of the counts above the background is measured in standard deviations, $\sigma = \sqrt{N_{\text{bg}}}$, where N_{bg} is given by the number of background events below the peaks

E_x [MeV]	g.s.	2.36(7)
E_R [MeV]	0.04(4)	2.32(7)
Γ [MeV]	<0.1	0.15
signif. [σ]	4.7	5.8
$d\sigma/d\Omega$ (5.1°) [nb/sr]	110 (35)	215(45)

configuration $(\pi 1p3/2 \otimes \nu 1d5/2)_{4^-}$ is the strongest peak in the low excitation energy region, with a weaker and broad underlying state at about the same excitation energy. If the same behaviour holds true for the ^{16}B nucleus, we can make a tentative assignment for the observed lowest resonance as $J^\pi = 4^-$ (we do not exclude that an unobserved 2^- state may be located at about the same place or even may form the ground state). The $\nu 2s1/2$ -shell, which is the dominant part in the ground state configuration, is now filled in the ^{16}B ground state by an additional neutron, and the second neutron is placed to the $\nu 1d5/2$ -shell giving rise to the much larger cross section. From the analogy to ^{14}B we do not expect a 3^- or 1^- state near the discussed $4^-/2^-$ states, one of which forms the ground state within the 40 keV decay energy range (with a preference for the 4^- state). In addition to the ground state peak, from Fig. 10, where the corresponding ^{16}B - and ^{14}B -states are presented one under the other, one can conclude that correspondence exists between the other high-lying excited states, too, and they probably have similar structure.

The ^{16}B -nucleus has 11 neutrons and, as mentioned earlier, by shell-model considerations the last neutron is expected to occupy the $1d5/2$ orbital. The $\ell = 2$ centrifugal barrier of nearly 3 MeV for the unbound neutron is much higher than the decay energy of only 40 keV. Thus due to the centrifugal barrier a considerable lifetime can be expected for the ^{16}B ground state. Our estimate is of the order of 10^{-17} s, taking for the barrier penetration a standard bound state potential including an $\ell \cdot s$ -term. The neutron has to tunnel through a barrier with a width of about 50 fm. Recently an attempt has been made to determine the lifetime of ^{16}B [32]. The nucleus ^{16}B has been produced by the fragmentation of a ^{17}C (52 MeV/A)-secondary beam on a ^{12}C -target. After a short flight-path, only 4 events reaching the detector could possibly be attributed to ^{16}B , but it could not be excluded that they came from some background processes. As a result, only an upper limit of the lifetime of ^{16}B was set: $\tau < 191$ ps. It is worthwhile noting, that having assumed that the last neutron occupies the $d5/2$ orbit, the authors of [32] give shell-model predictions for the lifetime of $3.7 \cdot 10^{-16}$ s for a decay energy of 10 keV, and $1.1 \cdot 10^{-13}$ s for a decay energy of 1 keV.

One of us (R.K.) would like to express her gratitude for the warm hospitality at HMI. Fruitful discussions with Yu.E.Penionzhkevich, D.V.Alexandrov, I.Mukha and A.A.Ogloblin are appreciated. This work was supported by NATO Linkage Grant no. 960375.

References

1. A.M. Poskanzer et al., Phys. Rev. Lett. **17**, 1271 (1966)
2. J.A. Musser and J.D. Stevenson, Phys. Rev. Lett. **53**, 2544 (1984)
3. J.D. Bowman et al., Phys. Rev. Lett. **31**, 614 (1973); Phys. Rev. C **9**, 836 (1974)
4. M. Langevin et al., Phys. Lett. B **150**, 71 (1985)
5. G. Audi and A.H. Wapstra, Nucl. Phys. A **565**, 1 (1993)
6. M. von Lucke-Petsch, Ph.D. thesis, Berlin, 1993; Th.Stolla, Ph.D. thesis, Berlin, 1995
7. F. Ajzenberg-Selove, Nucl. Phys. A **523**, 1 (1991), Nucl. Phys. A **433**, 1 (1985)
8. H.G. Bohlen et al., Z. Phys. A **320**, 237 (1985); also E.Adamides et al., Nucl. Phys. A **475**, 598 (1987)
9. D.J. Millener and D. Kurath, Nucl. Phys. A **255**, 315 (1975)
10. M.A. Firestone et al., Nucl. Phys. A **258**, 317 (1976)
11. A.A. Wolters et al., Phys. Rev. C **42**, 2053 (1990)
12. T. Anyas-Weiss et al., Phys. Rept. **12**, 201 (1974); W.D.M. Rae et al., Nucl. Phys. A **319**, 239 (1979)
13. K. Wang et al., Phys. Rev. C **53**, 1718 (1996)
14. R.A. Eramzhyan et al., Phys. Rep. **136**, 231 (1986)
15. F. Ajzenberg-Selove et al., Phys. Rev. C **17**, 1283 (1978)
16. R.Middleton and D.J.Pullen, Nucl. Phys. **51**, 50 (1964)
17. W. von Oertzen, Nucl. Phys. A **482**, 357c (1988); H.G. Bohlen et al., Progr. Part. Nucl. Phys. **42**, 17 (1999)
18. S. Nakayama et al., Nucl. Phys. A **507**, 515 (1990)
19. G.C. Ball et al., Phys. Rev. Lett. **28**, 1069, 1497 (1972)
20. G.T. Garvey and I. Kelson, Phys. Rev. Lett. **16**, 197 (1966)
21. G.C. Ball et al., Phys. Rev. Lett. **31**, 395 (1973)
22. F. Naulin et al., Proc. 4th Int. Conf. on NFFS, Helsingor 1981, ed. L.O.Skolen (CERN, Geneva, 1981) p. 376
23. E.K. Warburton and B.A. Brown, Phys. Rev. C **46**, 923 (1992)
24. H.W. Baer et al., Phys. Rev. C **28**, 761 (1983)
25. M. Belbot et al., Phys. Rev. C **56**, 3038 (1997); N. Aoi et al., Z. Phys. A **358**, 253 (1997)
26. M.A.C. Hotchkis et al., Nucl. Phys. A **398**, 130 (1983)
27. T.S. Bhatia et al., Phys. Lett. **76 B**, 562 (1978)
28. N.A.F.M. Poppelier et al., Phys. Lett. **157 B**, 120 (1985)
29. Yoshiko Kanada-Enyo and H. Horiuchi, Phys. Rev. C **52**, 647 (1995)
30. I. Tanihata, Progr. Part. Nucl. Phys. **35**, 505 (1995)
31. H.G. Bohlen et al., Nucl. Phys. A **583**, 775c (1995)
32. R.A. Kryger et al., Phys. Rev. C **53**, 1971 (1996)